

ARTICLES

A pH-Jump Reaction Studied by the Transient Grating Method: Photodissociation of *o*-Nitrobenzaldehyde

Jungkwon Choi, Noboru Hirota, and Masahide Terazima*

Department of Chemistry, Graduate School of Science, Kyoto University, Kyoto 606-8502, Japan

Received: April 14, 2000; In Final Form: October 12, 2000

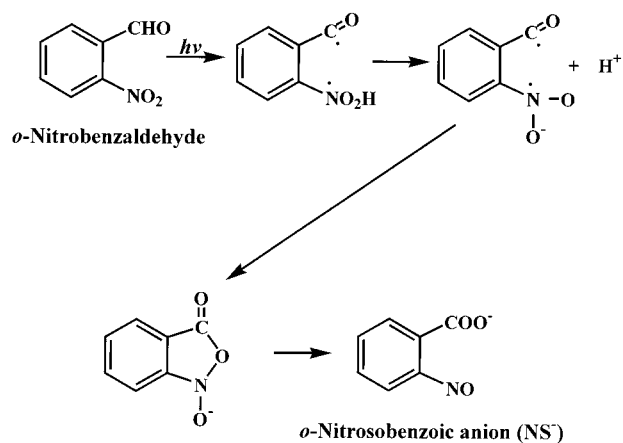
A proton-releasing photodissociation reaction of *o*-nitrobenzaldehyde is investigated by using the time-resolved transient grating method. The grating signal is very sensitive to the pH of the solution. The chemical species existing in the solution are identified from the diffusion constant of the species. For low-pH solutions, the grating signal due to the proton is observed clearly without any pH indicator. The origin of the signal is attributed to a pure volume grating, from which the partial molar volume of the proton can be determined accurately. The diffusion constant of the proton decreases with increasing the pH. This change is explained by the electrostatic interaction between the proton and the anion product, *o*-nitrosobenzoic anion. In an alkali solution, the hydroxyl ion is observed as the main species of the grating signal. By the quantitative measurement of the grating signal and the photoacoustic signal, the enthalpy change and the volume change of the reaction and the partial molar volumes of the proton are determined. This proton signal can be used to quantitatively measure the proton concentration change without any pH indicator.

1. Introduction

Photoinitiated proton-releasing reactions are important not only as prototype chemical reactions, but also they have many unique applications such as to the investigations of dynamics of pH-dependent phenomena, because these reactions can suddenly change the proton concentration (pH jump) in solution. For example, one of the interesting applications is the study of the kinetics of protein folding in solution. Since many protein structures are sensitive to pH, the dynamics between two structures under two different pH conditions can be initiated by the sudden changing of the pH, which is triggered by these reactions. Spectroscopic methods such as the transient grating (TG) can trace the dynamics of the energy, volume change, and diffusion constant of the protein folding. In such studies, the proton-releasing reaction is always overlapped with the target pH-dependent phenomena, and hence, the effect of the pH-jump reaction must be subtracted from the signal of the target reaction. For that purpose, the proton-releasing reaction must be characterized.

Aromatic alcohols such as naphthol¹ and its derivatives^{2,3} may be used for the pH-jump reaction, because the pK_a of the excited state is significantly different from that in the ground state. However, the period of the pH jump, which can be accomplished by such a molecule, is rather short because the system returns to the original state after the deactivation to the ground state. In this respect, the proton released by an irreversible reaction is useful for studying the pH-dependent phenomena in a long time period. A photodissociation reaction of *o*-nitrobenzaldehyde (*o*-NBA) is one of such reactions and, indeed, the reaction of *o*-NBA has been studied by the transient absorption⁴ and

SCHEME 1



photoacoustic (PA) methods^{5–7} so far. Very recently, this reaction was used to study the protein dynamics of apomyoglobin.⁸ In this paper, we study the photodissociation reaction of *o*-NBA by the time-resolved transient grating (TG) technique; one of powerful spectroscopic methods to reveal many properties of photochemical reactions.⁹

Upon the photoexcitation of *o*-NBA, the aci-form is rapidly produced through the intramolecular proton transfer reaction and the proton is dissociated to induce the nitronate anion in methanol and water (Scheme 1). Consequently the nitronate anion is converted to the *o*-nitrosobenzoic anion (NS^-) with a quantum yield of about 0.4 in methanol and water.⁴ In low-pH solutions, NS^- may be protonated to give the neutral form of *o*-nitrosobenzoic acid (NS).

One of the aims of this study is to clearly show the releasing of the proton during this reaction by the TG method. Although

* Author to whom correspondence should be addressed.

detection of the released proton should be important for the study of the pH reaction, direct optical detection is almost impossible because the optical absorption of the proton is not known even in the far UV region. Usually fluorescence from the proton-releasing molecule or pH indicators has to be used,^{2,10–11} but the fluorescence is not always detectable and the presence of the proton absorber (pH indicator) will change the amount and the dynamics of the proton. Using the TG method, we show that the creation of a proton can be easily detected as the grating signal (species grating) without any pH indicator. As far as we know, this is the first report of the proton detection by a spectroscopic method. Furthermore, since the TG signal is sensitive to the energy change as well as the structural change of macromolecules, such as proteins,¹² this technique is promising to apply to the protein folding problems in a wide time scale with the pH-jump reaction. Hence, it is important to characterize this reaction by the TG method. In addition, the TG method has a variety of advantages over the conventional techniques, in particular PA method, in studying this interesting reaction. First, the time window of the PA method is not wide enough for tracing the kinetics. The TG method can cover a very wide time scale, from nanoseconds to several tens milliseconds in this study. Second, since the observed PA signal consists of the thermal contribution as well as the volume contribution simultaneously, these components should be separated somehow. Usually, the PA intensities against various thermal expansion coefficients of the solution are plotted by the measurements at various temperatures, and the enthalpy change (ΔH) and the volume change (ΔV) are determined from the slope and the intercept of the plot.¹³ However, in this analysis, ΔH and ΔV are always assumed to be temperature independent. This assumption may not be correct for many reactions. In fact, Carcelli et al. found that ΔH and ΔV of the *o*-NBA photodissociation reaction are temperature dependent.⁷ Recently we reported that ΔV of some biological reactions are also temperature dependent.¹² As we showed previously¹² and also in this paper, using the TG and PA methods, it is not necessary to use this assumption: the energy change as well as the volume change can be detected at one temperature in one solvent under one pressure.¹⁴ Therefore, ΔH and ΔV from the TG-PA hybrid method will be more accurate.

2. Experimental Section

The experimental setup for the TG and PA experiments were similar to those reported before.^{14–16} The third harmonic of a Nd:YAG laser (Spectra-Physics Quantum-ray model GCR-170-10) with a 10 ns pulse was used as an excitation beam and a He–Ne laser beam (633 nm) or a photodiode laser (840 nm) as a probe beam. The diffracted probe beam was isolated from the excitation laser beam with a glass filter (Toshiba R-60) and a pinhole, detected by a photomultiplier tube (Hamamatsu R-928), and fed into a digital oscilloscope (Tetronix TDS-520). The TG signal was averaged by a microcomputer to improve a signal-to-noise (S/N) ratio. Photoacoustic signals were detected by a piezoelectric transducer (PZT). The signal was directly detected by the digital oscilloscope and averaged about 128 times. The TG signal, in particular, the grating signal due to the chemical species (species grating signal) was sensitive to the light irradiation. After several hundred shots of 5 μJ /pulse laser light to the sample solution (about 4 cm^3), the time profile of the signal changed gradually. The sample solution was changed to a fresh one after every 200 shots of the excitation laser pulses. The sample solution was prepared in a dark room just before the measurement.

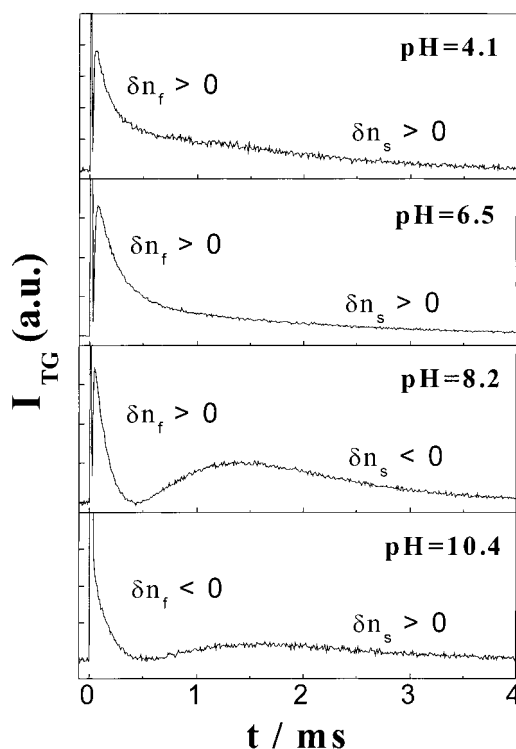


Figure 1. Time profiles of the TG signals after photoexcitation of *o*-NBA in various pH solutions.

The repetition rate of the excitation laser was about 1 Hz and the sample was gently stirred during measurement to prevent possible bleaching of the reactant and to dissipate photoproduct away from the excitation region. The size of the excitation beam at the sample position was ca. 1 mm \varnothing . The irradiated volume is small (typically ca. $4 \times 10^{-3} \text{ cm}^3$) compared with the entire volume of the sample solution. All measurements were carried out at room temperature. The absorbance of the samples in the transient grating and photoacoustic experiments was kept at about 0.5 at 355 nm, the excitation wavelength.

For a transient absorption (TA) experiment with a pH indicator, we used the same experimental setup as the TG measurement. The transmitted probe light intensity was detected by a photomultiplier and the time profile was recorded by the digital oscilloscope. The absorbance of *o*-NBA at 355 nm (the excitation wavelength) was about 0.5 for a 1-cm cell and the excitation energy of ca. 40 μJ /pulse was used.

o-Nitrobenzaldehyde (*o*-NBA), bromocresol green (BCG) and bromocresol purple (BCP) were obtained from Nacalai Tesque Inc. *o*-NBA was recrystallized from distilled water before use. Methanol, benzene, and distilled water (Nacalai Tesque Inc.) were used as received. The pH was adjusted with concentrated NaOH and HCl solutions.

3. Results and Discussion

3-1. Photodissociation of *o*-NBA. The TG signals after the photoexcitation of *o*-NBA in various pH solutions under the nitrogen-saturated condition are shown in Figure 1. Generally, the signal rises very fast (within 20 ns) and it decays with a rate constant that depends on q^2 (q : grating wave vector). Since this rate constant agrees well with $D_{\text{th}}q^2$ (D_{th} : thermal diffusivity of the solution), it is easy to identify it with the thermal grating signal, which is produced by the thermal energy coming from the nonradiative transition and the enthalpy change of the reaction. (In Figure 1, the thermal grating signal appears as an intense spike-like signal at $t \sim 0$.) The features of the signal

after the thermal grating depend on the solution (pH and the solvent). For example, the thermal grating signal decays to the baseline and a grow–decay curve is observed for low-pH solutions (Figure 1, pH = 4.1 and 6.5). For a higher-pH solution (pH = 8.2), after the thermal grating signal decays to the baseline, a slow-developing signal shows the grow–decay feature twice. For the pH = 10.4 solution, the thermal grating signal does not decay to the baseline but continuously decays slowly to the baseline and then shows a grow–decay curve. In the following, we interpret these changes of the grating signals by considering the chemical species involved in the reaction.

The TG signal intensity is proportional to the sum of the squares of the refractive index change and the absorbance change, which are induced by the spatially modulated photoexcitation. The change may be induced by the thermal energy (thermal grating) and by chemical species created (or depleted) after the photodissociation reaction of *o*-NBA (Scheme 1) (species grating). All the signals after the thermal grating signal should be attributed to the species grating signal. Since absorptions of any chemical species in this reaction are negligible at the probe wavelength (633 nm), the refractive index change is the main contribution to the signal. Although the features of the time development depend on the solution, we found that the temporal profile of the whole time range can be reproduced by a sum of three exponential functions in any solutions. All of the decay rate constants depend on q^2 , which fact indicates that the decay of the signal is governed by the diffusion process in the solution. Therefore, the TG signal can be expressed by

$$I_{\text{TG}}^{1/2} = \alpha |\delta n_{\text{th}}^0 \exp(-D_{\text{th}} q^2 t) + \delta n_{\text{f}}^0 \exp(-D_{\text{f}} q^2 t) + \delta n_{\text{s}}^0 \exp(-D_{\text{s}} q^2 t)| \quad (1)$$

where α is a constant, δn_{th}^0 , δn_{f}^0 , and δn_{s}^0 are initial refractive index changes of the thermal grating and the species gratings of the fast and slow decay components, respectively. D_{f} and D_{s} are the diffusion constants of the fast and slow decay components, respectively.

It is worth noting that, generally, the refractive index change of the thermal grating is negative ($\delta n_{\text{th}}^0 < 0$) and the interference dip between the thermal grating signal and species grating signal observed at pH ≤ 8.2 indicates that the dominant component of the species grating (the fast decay component) has a positive sign of the refractive index change ($\delta n_{\text{f}}^0 > 0$). The observed temporal profile of the species grating signal can be reproduced by a positive sign of δn_{s}^0 for pH = 4.1 and 6.5 solutions, but by a negative one for pH = 8.2. For a solution of pH = 10.4, the signs of δn_{f}^0 and δn_{s}^0 are negative and positive, respectively. The sign ($\delta n_{\text{f}}^0 > 0$) and the fast-decaying feature observed for pH = 4.1, 6.5, and 8.2 suggest that the chemical species which create δn_{f}^0 are the same.

We identify the chemical species by the sign of δn and the diffusion constant. Figure 2 shows plots of the decay rates of the fast- and slow-developing species grating signals against q^2 in the pH = 6.4 and 8.2 solutions. From the slopes of the plot, the diffusion constants of the fast and slow components in the pH = 4.1 solutions are determined to be $11.8 \times 10^{-9} \text{ m}^2 \text{ s}^{-1}$ and $0.45 \times 10^{-9} \text{ m}^2 \text{ s}^{-1}$, respectively. Considering the reaction scheme (Scheme 1), we expect that the proton (H^+), NS^- , and NS can contribute to the species grating signal. The diffusion constant of the fast component is remarkably larger than that expected for the anion (NS^-) or the neutral form (NS) of the *o*-nitrosobenzoic acid but rather close to the reported value of proton (D_{H^+}) in water ($(9.0\text{--}10) \times 10^{-9} \text{ m}^2 \text{ s}^{-1}$ at 25

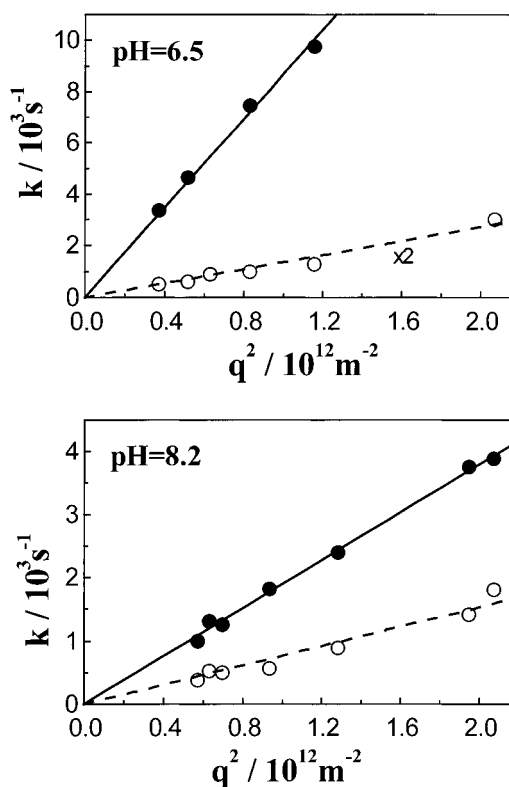


Figure 2. Plots of the decay rate constant (k) of the TG signal against q^2 in pH = 6.5 and 8.2 solutions and the least-squares fit by $k = Dq^2$ (solid line: fast component; dotted line: slow component).

TABLE 1: Diffusion Constants ($D/10^{-9} \text{ m}^2 \text{ s}^{-1}$) Measured after Photoexcitation of *o*-NBA^a

solvent	D_{H^+}	D_{NS^-}	D_{NS}	D_{OH^-}	D_{NBA}	D_{unknown}
aqueous: pH = 4.1	11.8	0.45				
aqueous: pH = 6.5	8.7	0.68				
aqueous: pH = 8.2	1.9				0.77	
aqueous: pH = 10.4				2.4		0.6
methanol	4.6	0.37				
benzene			1.5			

^a The subscripts denote the assignment of the diffusing species (H^+ : proton; NS^- : *o*-nitrosobenzoic anion; NS: *o*-nitrosobenzoic acid; OH^- : hydroxyl ion; NBA: *o*-nitrobenzaldehyde; unknown: unknown species.)

$^{\circ}\text{C}$).^{2,11,17–20} Considering the magnitude of D , we can assign the chemical species of the fast-decay component to H^+ definitely and the slow one to NS^- .

Here we consider the positive sign of δn_{f}^0 by the presence of the proton. The absorption change due to the creation of the proton is negligible. Therefore such a strong species grating signal is not expected by the presence of the proton only from the Kramers–Kronig relation. However, because of the electrostatic interaction with the water molecules, the local density of the water molecules becomes higher around the created proton (volume contraction as discussed later). This volume contraction increases the refractive index in the photoexcited region leading to $\delta n_{\text{f}}^0 > 0$. Therefore the strong TG signal of the proton is considered to be due to this volume contraction effect (volume grating). Indeed, the partial molar volume of the proton calculated from the signal intensity gives a reasonable volume of H^+ as will be shown in the next section. So far, the presence of the proton has been detected using pH indicators.^{21–23} However the presence of the pH indicator will change the dynamics of the proton. This TG detection is a new and sensitive method for the detection of the created proton. The q^2 plot

(Figure 2) shows that the created proton is persistent at least until several tens milliseconds.

It is interesting to note that with increasing the pH, D of the proton decreased to $1.9 \times 10^{-9} \text{ m}^2 \text{ s}^{-1}$ at pH = 8.2 (Table 1). This result may be interpreted in terms of the electrostatic interaction between the proton and the anion species. Since D of the anion species (NS^-) is much smaller than that of the proton, the interaction decreases D of the proton and, at the same time, increases D of NS^- . When the pH of the solution decreases, the proton in the solution becomes excess to shield the electrostatic interaction between the proton and NS^- , and D of the proton becomes close to that of the free proton. Furthermore, if the proton is in equilibrium with the anion (NS^-) very fast as described in eq 3,



the effective diffusion constant of the proton (D_{H^+}) should be expressed by

$$D_{\text{H}^+} = \frac{D_{\text{H}^+}^0 + \frac{D_{\text{NS}}[\text{NS}^-]}{K_{\text{NS}}}}{1 + \frac{[\text{NS}^-]}{K_{\text{NS}}}} \quad (4)$$

where $D_{\text{H}^+}^0$ is the diffusion constant of the free proton in water, D_{NS} is the diffusion constant of the NS, and K_{NS} is the equilibrium dissociation constant. This expression also predicts that D_{H^+} decreases with increasing $[\text{NS}^-]$ by increasing the pH of the solution. However, we found that the experimentally observed D_{H^+} in every pH solutions, in particular, the decrease of D_{H^+} in pH = 8.2 solution cannot be explained only by eq 4 with a single K_{NS} . Probably the electrostatic interaction as well as the chemical equilibrium (eq 3) simultaneously determine D_{H^+} . The diffusing species for the positive δn_s^o for the lower-pH solutions is attributed to NS^- , while the negative δn_s^o for pH = 8.2 solutions may come from the depletion of the parent molecule (*o*-NBA). The positive and negative δn represents the creation and the depletion of the molecules, respectively.

The TG signal measured in the high-pH solution (pH = 10.4) is clearly different from that in the low-pH solutions (pH \leq 8.2) as shown in Figure 1. Since the sign of δn_r^o is negative under this condition, the chemical species of this component cannot be the proton. From the slopes of the plot of the decay rate constant vs q^2 , D of the fast and slow component is determined to be $2.4 \times 10^{-9} \text{ m}^2 \text{ s}^{-1}$ and $0.6 \times 10^{-9} \text{ m}^2 \text{ s}^{-1}$, respectively. The diffusion constant of $2.4 \times 10^{-9} \text{ m}^2 \text{ s}^{-1}$ is too large for molecules with a size of *o*-NBA and NS. We attribute the chemical species of this large D to the hydroxyl ion (OH^-). The spatial modulation of the hydroxyl ion is created by the water formation reaction with the proton from *o*-NBA:



Because of this reaction, the concentration of OH^- in the light-illuminated region in the grating pattern decreases. Therefore the phase of the spatial modulation of the hydroxyl ion should be 180° shifted from the optical grating. Because of the volume expansion of the reaction 5, the sign of refractive index change should be negative ($\delta n_r^o < 0$). D of the species ($2.4 \times 10^{-9} \text{ m}^2 \text{ s}^{-1}$) is smaller than the reported D of OH^- ($5.3 \times 10^{-9} \text{ m}^2 \text{ s}^{-1}$ at 25°C).¹⁷ Similar to the reduction of D_{H^+} described above, this large reduction may be also explained by the electrostatic

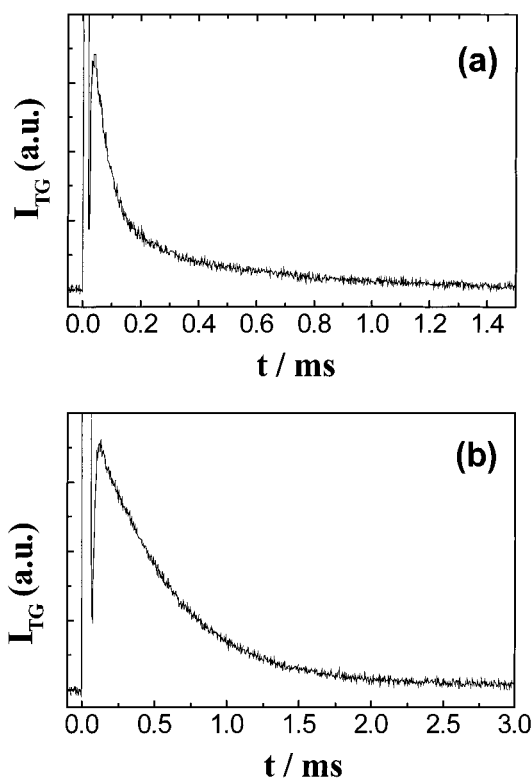


Figure 3. Time profiles of the TG signals after photoexcitation of *o*-NBA in methanol (a) and in benzene (b).

interaction between OH^- and ionic species in this solution but the exact origin of this reduction is not known.

The origin of the slow component ($\delta n_s^o > 0$) at pH = 10.4 is not clear at present, but we tentatively assign the chemical species of the slow component at pH = 10.4 to NS^- .

In addition, the TG signals after the photochemical reaction of *o*-NBA in organic solvents such as methanol and benzene were measured as shown in Figure 3. The species grating signals observed after the decay of the thermal grating signal are very weak compared with those in aqueous solutions. The TG signal observed in methanol is very similar to those in pH = 4.1 and 6.5, suggesting that the fast component is attributed to the proton and the slow component to the *o*-nitrosobenzoic anion (NS^-). From the slopes of the plots of the decay rate constants vs q^2 , D of the proton and NS^- in methanol are estimated to be $4.6 \times 10^{-9} \text{ m}^2 \text{ s}^{-1}$ and $0.37 \times 10^{-9} \text{ m}^2 \text{ s}^{-1}$, respectively. The measured D_{H^+} in methanol is two times smaller than that in water. This small D_{H^+} may be due to the weak hydrogen-bonding ability of methanol. A decrease in the hydrogen-bonding ability of the solvent should decrease D_{H^+} by the loss of hydrogen-bond bridges for migration. In contrast to the species grating signal observed in polar solvents, the species grating signal in benzene can be well fitted with a single-exponential function and the diffusion constant is estimated to be $1.5 \times 10^{-9} \text{ m}^2 \text{ s}^{-1}$. Since the polarity of benzene is further smaller than methanol and water, the dissociation of the proton observed in the process of the photochemical reaction of *o*-NBA does not take place. Therefore we think that the measured species grating signal originates from the *o*-nitrosobenzoic acid (NS).

3-2. Enthalpy and Volume Changes. The magnitude of δn_{th} is given by

$$\delta n_{\text{th}} = \frac{dn}{dT} \frac{hv\phi W}{\rho C_p} \Delta N \quad (6)$$

$$\phi = \frac{hv - \Phi\Delta H}{hv}$$

where dn/dT is the temperature dependence of the refractive index, hv is the photon energy of the excitation energy (337kJ/mol), Φ is the quantum yield of the nonradiative transition, and W is the molecular weight. ΔH is defined by the enthalpy change from the reactant to the product. The enthalpy change of this photodissociation reaction can be determined by the quantitative measurement of the thermal grating intensity. When the excitation laser power increases, the thermal grating signal intensity increases almost linearly, but the species grating intensity is saturated at rather low power (10 μ J/pulse). We think that the different power dependence is due to the sequential transient absorptions by the reaction products within the laser pulse. The extra-photoexcitation will increase the released thermal energy but not the species grating signal. We quantitatively measured the TG intensity within the weak laser power region, in which the square of the species grating signal intensity is linear to the excitation laser power.

The thermal grating intensities of *o*-NBA in the pH = 6.5, 8.2 and methanol solutions are compared with that of the reference sample, BCP, which gives rise to only the thermal grating signal with a unit quantum yield of the nonradiative transition within the pulse width of the excitation laser. ΔH was calculated from eqs 6 and 7:

$$\Phi\Delta H = 337 \text{ kJ/mol} \cdot \left(1 - \frac{\delta n_{\text{th}}(\text{sample})}{\delta n_{\text{th}}(\text{reference})}\right) \quad (7)$$

where $\delta n_{\text{th}}(\text{sample})$ and $\delta n_{\text{th}}(\text{reference})$ are the refractive index changes of the thermal grating of the sample and reference, respectively.

We found that the thermal grating intensity of *o*-NBA is much larger than that of the reference sample. The larger thermal grating intensity indicates that the reaction is exothermic. From the thermal grating intensity, $\Phi\Delta H$ in the pH = 6.5 and 8.2 solutions are determined as $-52.5 \pm 0.5 \text{ kJ mol}^{-1}$ and $-53.5 \pm 0.5 \text{ kJ mol}^{-1}$, respectively. Using the reported quantum yield, $\Phi = 0.4$, ΔH at pH = 6.5 and 8.2 are estimated to be -131 and -134 kJ mol^{-1} , respectively.

The measured ΔH at pH = 6.5 is significantly larger than that reported by Carcelli et al.⁷ They reported ΔH for the photolysis of *o*-NBA in neutral aqueous solutions ([NaCl] = 100mM) as $-88.5 \text{ kJ mol}^{-1}$ by the temperature dependence of the photoacoustic (PA) signal intensity in a range of 4–15 $^{\circ}\text{C}$. In the PA method, ΔH and ΔV are always assumed to be temperature independent. If they are not, the signals from the thermal and volume contributions are significantly mixed and the values are not accurate. Despite this assumption, they actually reported anomalous temperature dependence of ΔH . This fact indicates that the previous analysis may not be correct. Therefore, the difference between ΔH from the TG and from the PA methods may be due to this temperature-dependent ΔH . (The thermal contribution can be isolated without any assumption by the TG method.²⁴)

In higher-pH solutions, the TG signal intensity is very sensitive to the light irradiation. After a small number of laser shots, the time profile of the TG signal changes. It is known that *o*-NBA is unstable in an alkali solution.²⁵ The light sensitivity of *o*-NBA in the higher-pH solution may be related to this additional reaction. Hence we could not measure the TG intensity quantitatively.

ΔH determined in methanol is $-28.3 \text{ kJ mol}^{-1}$, which is much smaller than those in aqueous solutions, indicating that NS^- is more stable in water than in methanol (Table 1).

TABLE 2: Enthalpy (ΔH) and Volume Changes (ΔV) on the Photodissociation Reaction of *o*-NBA in Aqueous Solutions and Methanol and the Partial Molar Volume of the Proton (\bar{V}_{H^+})

	$\Delta H/\text{kJ/mol}$	$\Delta V/\text{mL/mol}$	$\bar{V}_{\text{H}^+}/\text{mL/mol}$
pH = 6.5	-131	-5.3	-6.04
pH = 8.2	-134	-7.5	-7.45
pH = 10.4	-132 ^{a)}	15.6	
methanol	-28.3	22.9	

^{a)} The mean value of ΔH measured in pH = 6.5 and 8.5.

$\Phi\Delta V$ is measured from the PA intensity using ΔH determined from the TG experiment. The temporal profile of the PA signal of the *o*-NBA sample is almost identical to that of the reference sample. We did not observe any temporal delay in the signal and this fact is consistent with the fast rising of the TG signal at all pH (See Section 3.1). Indeed, Bonetti et al. reported that the volume contraction at neutral pH is completed within a few nanoseconds.⁵ Furthermore, considering the rate constant for the ionic equilibrium of water, $k_1 = 1.4 \times 10^{11} \text{ M}^{-1} \text{ s}^{-1}$ and $k_2 = 2.4 \times 10^{-5} \text{ s}^{-1}$ (see eq 5),¹⁷ at pH = 10.4 the neutralization reaction (volume expansion) between photodissociated proton and hydroxyl ion is completed within ca. 30 ns. Since this kinetics is very fast compared with our PA experimental resolution, we did not deconvolute the photoacoustic signals. In this case, the PA intensity (I_{PA}) is given by

$$I_{\text{PA}} = A' \Delta N \left[(hv_{\text{ex}} + \Phi\Delta H) \cdot \left(\frac{W\beta}{\rho \cdot C_p} \right) + \Phi\Delta V \right] \quad (8)$$

where A' is a proportional constant which includes the sensitivity of the apparatus, ΔN is a number of the reactive molecules in the unit volume, and β is the thermal expansion coefficient.

From the acoustic signal intensities of the sample and the reference sample, and with ΔH obtained from the TG experiment, $\Phi\Delta V$ in pH = 6.5 and 8.2 solutions can be determined as -2.1 ± 0.1 and $-3.0 \pm 0.1 \text{ mL/mol}$, respectively. Using the quantum yield, $\Phi = 0.4$, we obtain ΔV in pH = 6.5 and 8.2 to be -5.3 and -7.5 mL/mol , respectively. The ΔV corresponds to the molecular volume change and the solvation of the photogenerated ions (Table 2). These values are consistent with the previously reported values of -5.2 mL/mol at pH = 6.7⁵ and -7.1 mL/mol in neutral aqueous solutions ([NaCl] = 100 mM).⁷

Not only the reaction volume, but also the partial molar volume (\bar{V}_i) of molecule i in a chemical reaction can be determined from the grating signal intensity in some cases.¹⁴ The refractive index change due to the creation of i species (δn_{spe}^i) consists of the absorption term (population grating: δn_{pop}^i) and the volume term (volume grating: δn_{v}^i) ($\delta n_{\text{spe}}^i = \delta n_{\text{pop}}^i + \delta n_{\text{v}}^i$). If we can quantitatively estimate the magnitude of δn_{v}^i , we can calculate \bar{V}_i from a relation of¹⁴

$$\delta n_{\text{v}}^i = \frac{(n_0^2 + 2)^2 \alpha_{\text{solvent}}}{18n_0 \epsilon_0 \bar{V}_{\text{solvent}}} \Delta N \bar{V}_i \quad (9)$$

where α_{solvent} is the molecular polarizability of the solvent, n_0 is the unperturbed refractive index of solution, and ϵ_0 is the vacuum permittivity. In this case, since the absorption of the proton can be neglected, we may neglect the contribution of δn_{pop} in the signal, too. Thus, the partial molar volume of the proton (\bar{V}_{H^+}) can be calculated from the intensity of the species grating of the proton and eq 9. The \bar{V}_{H^+} values at pH = 6.5 and 8.2 are determined to be -6.04 and -7.45 mL/mol , respectively. These values are consistent with the previously reported \bar{V}_{H^+}

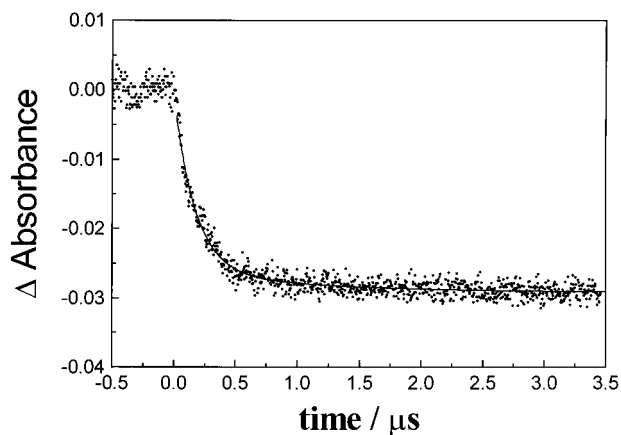


Figure 4. Time profile of the absorbance change of BCG^- probed at 633 nm following the photolysis of *o*-NBA and 10 μM BCG in pH 6.5 aqueous solution. The solid line denotes the fitted curve by a single-exponential function.

values in water at 25 °C (5.4–7.6 mL/mol).^{26–30} This good agreement supports the negligible contribution of the population term for H^+ .

On the other hand, using the mean value of ΔH measured at pH = 6.5 and 8.2, a large ΔV of 15.6 mL/mol in pH = 10.4 is estimated, indicating that, as mentioned above, the neutralization reaction of the photodissociated proton with hydroxyl ion leading to the water formation takes place substantially. Indeed, this ΔV is close to the sum of the volume change obtained at pH = 6.5 and the reported volume change of the water formation $\text{H}^+ + \text{OH}^- \rightarrow \text{H}_2\text{O}$, $\Delta V = 22.4 \text{ cm}^3/\text{mol}$.^{30–33} On the other hand, ΔV in methanol is estimated to be 22.9 mL/mol that is much larger than those in water solutions (Table 2).

3-3. pH Jump with a pH Indicator. In some cases of the proton-releasing experiments, the kinetics of the proton was detected by using pH indicators. Here we studied the TG signal of the photodissociation of *o*-NBA in the presence of a pH indicator for comparison. We used BCG as the pH indicator. pK_a of this indicator is 4.7 and the deprotonated form of BCG (BCG^-) shows a strong absorption band at 610 nm in pH > 5. Since the change in absorbance of BCG^- means the protonation of BCG^- induced by the pH-jump reaction, the change of the pH can be calculated from the absorbance of BCG^- . As shown in Figure 4, the protonation of BCG^- is completed within several hundred nanoseconds (ca. 300 ns) and is persistent until a few seconds. Using the reported molar extinction coefficient of BCG^- at 633 nm, $\epsilon = 33000 \text{ M}^{-1} \text{ cm}^{-1}$,³⁴ the increase of the proton concentration is calculated to be ca. $2.0 \times 10^{-6} \text{ M}$.

On the other hand, the TG signal of *o*-NBA became stronger by an addition of the pH indicator, BCG (10 μM) because of the absorbance changes of the probe light. The TG signal in this case should come from the absorbance change as well as the refractive index change and the TG signal should be now expressed by

$$I_{\text{TG}}^{1/2} = \alpha |\delta n_{\text{th}}^{\circ} \exp(-D_{\text{th}} q^2 t) + \delta n_{\text{f}}^{\circ} \exp(-D_{\text{f}} q^2 t) + \delta n_{\text{s}}^{\circ} \exp(-D_{\text{s}} q^2 t)| + \beta |\delta k_{\text{f}}^{\circ} \exp(-D_{\text{f}} q^2 t) + \delta k_{\text{s}}^{\circ} \exp(-D_{\text{s}} q^2 t)| \quad (10)$$

where β is a constant and $\delta k_{\text{f}(\text{s})}^{\circ}$ is the absorption changes by the reaction. In this case, there are too many adjustable parameters to be determined uniquely by the signal fitting. To avoid the contribution of the absorbance change in the TG signal, we monitored the TG signal using a photodiode laser

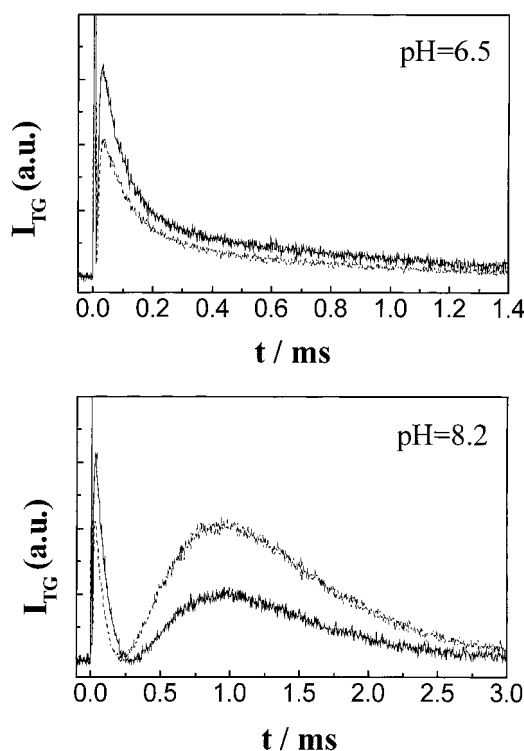


Figure 5. Time profiles of the TG signals after the photoexcitation of *o*-NBA in absence (solid line) and presence (dotted line) of the pH indicator ($[\text{BCG}] = 10 \mu\text{M}$) in pH = 6.5 and pH = 8.2 solutions.

TABLE 3: Diffusion Constants ($D/10^{-9} \text{ m}^2 \text{ s}^{-1}$) Measured after Photoexcitation of *o*-NBA in the Absence and Presence of the pH Indicator

		D_{H^+}	D_{NS^-}	D_{NBA}
pH = 6.5	without BCG	8.8	0.63	
	with BCG	8.2	0.77	
pH = 8.2	without BCG	2.0		0.78
	with BCG	1.4		0.86

(840 nm) as the probe beam. The TG signal of *o*-NBA in the presence of the pH indicator is very similar to that in the absence of the pH indicator as depicted in Figure 5, except the relative intensity of the fast-decaying component. This similarity indicates that the chemical species involved in the species grating signal are the same regardless of the presence of the pH indicator. That is, the chemical species of the fast-decay component observed in the pH = 6.5 and 8.2 solutions is attributed to the proton and the slow component corresponding to NS^- and the parent molecule (*o*-NBA), respectively. The weaker fast-decaying component suggests that the proton is absorbed by the pH indicator. The diffusion constants measured in the presence of the pH indicator are also similar to those in the absence of the pH indicator within experimental uncertainty. The diffusion constant of each chemical species in the absence and the presence of the pH indicator is listed in Table 3.

4. Conclusions

We studied the proton-releasing reaction of *o*-NBA in various solvents using the transient grating (TG) technique. The TG signal is found to be sensitive to the pH of the solution and the pH dependence is explained in terms of the chemical species existing in the solution. In low-pH solutions, the creation of the proton is clearly detected as a strong species grating signal, which decays with a rate constant of $D_{\text{H}^+} q^2$. As far as we know, this is the first detection of proton by the TG technique. The

positive refractive index change is explained by the volume contraction by the presence of the proton. The partial molar volume of the proton (-6 to -7 mL/mol) was determined from the grating intensity. Using this intensity, we can quantitatively measure the concentration of the proton (amount of the pH jump) without any pH indicator. In a higher-pH solution, the time profile of the TG signal changes dramatically. The chemical species, which gives rise to the strong and fast-decaying species grating signal in a high-pH solution is attributed to OH^- . The enthalpy change and the reaction volume of the photodissociation reaction are determined without temperature variation. The negative volume change (contraction) in lower-pH solutions is due to the electrostriction by the creation of the ionic species. At higher pH, the reaction volume changes to positive (expansion), which is mainly due to the water formation. These fundamental properties of this reaction will be a basis for studying pH-dependent phenomena using the pH-jump method and will be published in future.

Acknowledgment. A part of this study was support by the Grant-in-Aid (No. 10440173) and the Grant-in-Aid on Priority Area of "Chemical Reaction Dynamics in Condensed Phase" (10206202) from the Ministry of Education, Science, Sports and Culture in Japan.

References and Notes

- (1) Weller, M. *Prog. React. Kinet.* **1961**, *1*, 187.
- (2) Solntsev, K. M.; Huppert, D.; Agmon, N. *J. Phys. Chem. A* **1999**, *103*, 6984.
- (3) Huppert, D.; Tolbert, L. M.; Linares-Samaniego, S. *J. Phys. Chem. A* **1997**, *101*, 4602.
- (4) George, M. V.; Scaiano, J. C. *J. Phys. Chem.* **1980**, *84*, 492.
- (5) Bonetti, G.; Veccli, A.; Viappiani, C. *Chem. Phys. Lett.* **1997**, *169*, 268.
- (6) Viappiani, C.; Abbruzzetti, S.; Small, J. R.; Libertini, L. J.; Small, E. W. *Biophys. Chem.* **1998**, *73*, 13.
- (7) Carcelli, M.; Pelagatti, P.; Viappiani, C. *Isr. J. Chem.* **1998**, *38*, 213.
- (8) Abbruzzetti, S.; Crema, E.; Masino, L.; Veccli, A.; Viappiani, C.; Small, J. R.; Libertini, L. J.; Small, E. W. *Biophys. J.* **2000**, *78*, 405.
- (9) Terazima, M. *Adv. Photochem.* **1998**, *24*, 255.
- (10) Gutman, M.; Huppert, D.; Pines, E. *J. Am. Chem. Soc.* **1981**, *103*, 3709.
- (11) Pines, E.; Huppert, D. *J. Phys. Chem.* **1983**, *87*, 4471.
- (12) Sakakura, M.; Yamaguchi, S.; Hirota, N.; Terazima, M. Submitted.
- (13) Hung, R. R.; Grabowski, J. J. *J. Am. Chem. Soc.* **1992**, *114*, 351.
- (14) Hara, T.; Hirota, N.; Terazima, M. *J. Phys. Chem.* **1996**, *100*, 10194.
- (15) Terazima, M.; Hara, T.; Hirota, N. *Chem. Phys. Lett.* **1995**, *246*, 577.
- (16) Terazima, M.; Azumi, T. *Bull. Chem. Soc. Jpn.* **1990**, *63*, 741.
- (17) Atkins, P. W. *Physical Chemistry*, 5th ed.; Oxford University Press: Oxford, 1996.
- (18) Biondi, C.; Belligi, L. *Chem Phys.* **1981**, *62*, 145.
- (19) Elliot, A. J.; McCracken, D. R.; Buxton, G. V.; Wood, N. D. *J. Chem. Soc., Faraday Trans.* **1990**, *88*, 1539.
- (20) Thomsen, C. L.; Madsen, D.; Keiding, S. R.; Thøgersen, J.; Christiansen, O. *J. Chem. Phys.* **1999**, *110*, 1539.
- (21) Gutman, M.; Huppert, D.; Pines, E. *J. Am. Chem. Soc.* **1981**, *103*, 3709.
- (22) Pines, E.; Huppert, D. *J. Phys. Chem.* **1983**, *87*, 4471.
- (23) Nachliel, E.; Gutman, M. *J. Am. Chem. Soc.* **1988**, *110*, 2629.
- (24) Yamaguchi, S.; Hirota, N.; Terazima, M. *Chem. Phys. Lett.* **1998**, *286*, 284.
- (25) March, J. *Advanced organic chemistry*; John Wiley & Sons, Inc. press, **1992**, 1233.
- (26) Couture, A. M.; Laidler, K. J. *Can. J. Chem.* **1956**, *34*, 1209.
- (27) Stokes, R. H.; Robinson, R. A. *Trans. Faraday Soc.* **1957**, *53*, 301.
- (28) Millero, F. J.; Drost-Hansen, W. *J. Phys. Chem.* **1968**, *72*, 1758.
- (29) Zana, R.; Yeager, E. *J. Phys. Chem.* **1966**, *70*, 954.
- (30) Zana, R.; Yeager, E. *J. Phys. Chem.* **1967**, *71*, 521.
- (31) Asano, T.; Le Noble, W. J. L. *Chem. Rev.* **1978**, *78*, 407.
- (32) Van Eldic, R.; Asano, T.; Le Noble, W. J. L. *Chem. Rev.* **1989**, *89*, 549.
- (33) Millero, F. J.; Hoff, E. V.; Cahn, L. *J. Solid Chem.* **1972**, *1*, 309.
- (34) Viappiani, C.; Bonetti, G.; Carcelli, M.; Ferrari, F.; Sternieri, A. *Rev. Sci. Instrum.* **1998**, *69*, 270.